

1 **Paper pulp-based adsorbents for the removal of pharmaceuticals from**
2 **wastewater: a novel approach towards diversification**

3 *Gonçalo Oliveira^a, Vânia Calisto^{b*}, Sérgio M. Santos^c, Marta Otero^d, Valdemar I. Esteves^b*

4

5 ^a Department of Chemistry, University of Aveiro, Campus de Santiago, 3810-193 Aveiro,
6 Portugal

7 ^b Department of Chemistry and CESAM (Centre for Environmental and Marine Studies),
8 University of Aveiro, Campus de Santiago, 3810-193 Aveiro, Portugal

9 ^c Department of Chemistry and CICECO (Aveiro Institute of Materials), University of Aveiro,
10 Campus de Santiago, 3810-193 Aveiro, Portugal

11 ^d Department of Environment and Planning and CESAM (Centre for Environmental and Marine
12 Studies), University of Aveiro, Campus de Santiago, 3810-193 Aveiro, Portugal

13

14 *Corresponding author: E-mail address: vania.calisto@ua.pt

15

16 **Abstract**

17 In this work, two pulps, bleached (BP) and raw pulp (RP), derived from the paper production
18 process, were used as precursors to produce non-activated and activated carbons (ACs). In the
19 case of non-ACs, the production involved either pyrolysis or pyrolysis followed by acid
20 washing. For ACs production, the pulps were impregnated with K_2CO_3 or H_3PO_4 , and then
21 pyrolysed and acid washed. After production, the materials were physically and chemically
22 characterized. Then, batch adsorption tests on the removal of two pharmaceuticals (the anti-
23 epileptic carbamazepine (CBZ) and the antibiotic sulfamethoxazole (SMX)) from ultra-pure
24 water and from Waste Water Treatment Plant (WWTP) effluents were performed. In ultra-pure
25 water, non-ACs were not able to adsorb CBZ or SMX while ACs showed good adsorption
26 capacities. In WWTP effluents, although ACs satisfactorily adsorbed CBZ and SMX, they
27 showed lower adsorption capacities for the latter. Tests with WWTP effluents revealed that the
28 best adsorption capacities were achieved by carbons produced from BP and activated with
29 H_3PO_4 : $92 \pm 19 \text{ mg g}^{-1}$ for CBZ and $13.0 \pm 0.6 \text{ mg g}^{-1}$ for SMX. These results indicate the
30 potential of paper pulps as precursors for ACs that can be applied in wastewater treatment.

31

32 **Keywords:** Emerging contaminants; Adsorption; Activated carbons; Water treatment; Raw
33 pulp; Bleached pulp.

34

35

36

37

38

39

40

41

42

43 **1. Introduction**

44 The consumption of pharmaceuticals has been increasing considerably over the last
45 decades and with this, their concentration in the environment, mainly aquatic, has grown up too,
46 reaching the $\mu\text{g L}^{-1}$ levels (Jones et al., 2005). The main pathway for the entrance of
47 pharmaceuticals into the environment is the Wastewater Treatment Plants (WWTP) effluents
48 discharge. There is a limited capacity to remove pharmaceuticals from urban wastewaters due to
49 their resistance to conventional treatments. Microorganisms cannot metabolize most drugs as
50 source of carbon (Ren et al., 2018), resulting in the release of contaminated effluents into the
51 aquatic resources that ultimately supply the population (Bahlmann et al., 2014, 2012; Calisto et
52 al., 2011; Rivera-Utrilla et al., 2013)). This fact has been worrying the scientific community,
53 causing the search for new options to solve this serious environmental problem. One of the
54 proposed solutions relies on the implementation of tertiary treatments in WWTP using
55 adsorbent materials, most commonly activated carbons (ACs). In fact, it is well known that
56 adsorption is a very versatile and efficient method to remove contaminants from the
57 environment (Bansal and Goyal, 2005).

58 ACs are very efficient in adsorption processes, mainly due to very high specific surface
59 areas, most frequently between 800 and 1500 $\text{m}^2 \text{g}^{-1}$ (Bansal and Goyal, 2005). However, their
60 production is quite expensive since the most common used raw materials are petroleum coke, a
61 product obtained during the oil refining process, and charcoal. Also, these precursors constitute
62 non-renewable resources and originate environmental problems (Wei and Yushin, 2012). The
63 production of adsorbent materials from alternative and renewable raw materials is becoming
64 more and more important in line with the need to adopt processes that promote a more
65 sustainable economy. Adsorbents have been developed from low-cost bio-based raw materials,
66 from diverse origins (Babel, 2003), being agricultural residues the most common type of
67 precursor: cocoa (Saucier et al., 2015) and coconut (Jain et al., 2015) shells, cherry stones
68 (Nowicki et al., 2015), potato peels (Kyzas and Deliyanni, 2015), Isabel grape bagasse (Antunes
69 et al., 2012), coffee residues and almond shells (Flores-Cano et al., 2016), among many others.
70 Adsorbents were also produced from industrial residues like macroalgae waste originated from

71 agar-agar industry (Ferrera-Lorenzo et al., 2014), carbon residues from woody biomass
72 gasification (Maneerung et al., 2016), cellulose sludge (Orlandi et al., 2017) and sewage sludge
73 of industrial laundries (Silva et al., 2016). One type of substrate that has also been exploited is
74 the sludge resulting from wastewater treatment in the pulp and paper industry (Calisto et al.,
75 2015, 2014; Ferreira et al., 2016; Jaria et al., 2017, 2015; Khalili et al., 2002; Li et al., 2011).
76 Such sludge is produced at a rate of eleven million tons per year in Europe alone (Monte et al.,
77 2009) and its management is an issue of concern for the paper industry. Beyond the abundance
78 of this sludge, it also presents very interesting characteristics as adsorbent precursor, namely
79 high percentage of carbon and volatiles (Azargohar and Dalai, 2008), which are typical of
80 lignocellulosic materials. Raw (RP) and bleached paper pulp (BP) have very similar chemical
81 composition to primary paper mill sludge. Therefore, it could be expected that RP and BP may
82 also have good potential to be used as precursors to generate adsorbents, presenting some
83 advantages in comparison to sludge: (i) their composition is more stable over time; and (ii) they
84 have less inorganic content, which may allow to produce carbons with higher yield and organic
85 carbon content.

86 The European pulp and paper industry is facing big challenges mainly related to the
87 consumption decay (which is expected to continue due to the digitalization) and to the sector's
88 objectives for the 2050 Roadmap towards a low-carbon bio-economy (Confederation of
89 European Paper Industries, 2014; European Commission, 2013; Presas, 2011). Innovation is
90 essential to cope with these challenges, this involving progressing towards the diversification
91 and exploitation of new businesses, the development of breakthrough technologies, novel
92 products, and applications based on cellulose fibre that generate more added value. In this
93 context, this manuscript aims to evaluate, for the first time, the adequacy of RP and BP from the
94 paper industry as alternative and sustainable precursors of carbonaceous adsorbents. For this
95 purpose, RP and BP were subjected to pyrolysis or pyrolysis combined with chemical
96 activation. The resulting materials were subjected to extensive physico-chemical
97 characterization and applied to the removal of carbamazepine (CBZ) and sulfamethoxazole
98 (SMX) both from ultra-pure water and from the secondary effluent of a local WWTP to assess

99 the performance of the produced materials in real matrixes. CBZ and SMX were selected
100 because, belonging to two different groups and presenting distinct chemical characteristics, both
101 have large consumption patterns and have been found in natural waters: CBZ is an antiepileptic
102 drug, with a very large global consumption and environmental persistency (Clara et al., 2004),
103 widely detected in aqueous systems (Bahlmann et al., 2014, 2012; Calisto et al., 2011); SMX is
104 the most representative antibiotic of the sulphonamides group, poses bacteriostatic activity, is
105 widely administered in human and veterinary medicine and has been found in water systems
106 (Johnson et al., 2015; Larcher and Yargeau, 2012).

107

108 **2. Experimental section**

109 **2.1. Production of carbon adsorbents**

110 The precursors used in the production of carbon adsorbents were RP and BP, provided
111 by a kraft elemental chlorine free pulp factory, operating using *Eucalyptus globulus* wood. The
112 pulp manufacturing process comprises three main steps: cooking, washing and bleaching (aimed
113 to increase the degree of whiteness by removing or modifying chromophore groups present in
114 the pulp structure). RP and BP were collected before and after the bleaching process,
115 respectively. From the two air dried pulps, twelve different carbons were produced: six from RP
116 and six from BP. Within the six carbons produced from each precursor, two were only
117 pyrolysed (RP500 and RP800 produced from RP; BP500 and BP800 from BP), two other were
118 pyrolysed and then acid washed with HCl 1.2 M (RP500-HCl and RP800-HCl from RP; BP500-
119 HCl and BP800-HCl from BP) and two were activated (either with K₂CO₃ or with H₃PO₄),
120 pyrolysed and acid washed (RP800-HCl-K₂CO₃ and RP800-HCl-H₃PO₄ from RP; BP800-HCl-
121 K₂CO₃ and BP800-HCl-H₃PO₄ from BP). For the activation procedure, the pulp fibres were
122 impregnated with the activating agent in a ratio of 1:1 (w/w). For the carbons activated with
123 K₂CO₃, the activating agent was dissolved in distilled water with a proportion of 3:10 (w/v) and
124 for H₃PO₄ activation, the activating agent was diluted in a ratio of 1:8 (v/v). In both cases, the
125 pulp was impregnated for 1 h with the activating agent solution, using an ultrasonic bath and

126 then dried at room temperature. The dried pulps (alone or impregnated with the activating
127 agent) were then placed in porcelain crucibles and pyrolysed under nitrogen flow in a furnace
128 muffle that was heated at a rate of $10\text{ }^{\circ}\text{C min}^{-1}$ up to $500\text{ }^{\circ}\text{C}$ or $800\text{ }^{\circ}\text{C}$, temperatures which were
129 maintained for 150 minutes. Then, also under nitrogen flow, the furnace was allowed to cool
130 until room temperature. After pyrolysis, the ACs and two non-ACs from each pulp were acid
131 washed with HCl 1.2 M (1 L of HCl 1.2 M to 30 mg of carbon adsorbent) and washed with
132 distilled water until washing water reaching neutral pH. After that, all carbons were dried in an
133 oven at $105\text{ }^{\circ}\text{C}$ for 24 h and crushed mechanically.

134

135 **2.2. Physical and chemical characterization of raw materials and carbon adsorbents**

136 **2.2.1. Total organic carbon (TOC)**

137 TOC was determined for both precursors and for all carbon adsorbents by the difference
138 between total carbon (TC) content and inorganic carbon (IC) content, which were obtained
139 through a TOC analyser (TOC-VCPH Shimadzu, solid sample module SSM-5000A). Carbon
140 content was determined as the average of three replicates.

141 **2.2.2. Thermogravimetric and proximate analysis**

142 The thermogravimetric analysis (TGA) and proximate analyses were made for the
143 precursors and for the produced carbon adsorbents, respectively, and were carried out in a
144 thermogravimetric balance Setsys Evolution 1750, Setaram, TGA mode (S type sensor).
145 Standard methods to determine the moisture (UNE 32002) (AENOR, 1995), volatile matter
146 (UNE 32019) (AENOR, 1985) and ash content (UNE 32004) (AENOR, 1984) were employed.
147 The fixed carbon was determined as the remaining fraction after ash and volatile matter (at dry
148 basis) determination. The experimental procedure for TGA consisted of the sample heating,
149 under nitrogen atmosphere, from room temperature to $105\text{ }^{\circ}\text{C}$ (heating rate of $10\text{ }^{\circ}\text{C min}^{-1}$);
150 sample was kept at this temperature until total stabilization of the weight (approximately 30
151 min); next, temperature was increased from 105 to $950\text{ }^{\circ}\text{C}$ ($10\text{ }^{\circ}\text{C min}^{-1}$), keeping the sample at
152 $950\text{ }^{\circ}\text{C}$ until total stabilization of the weight (approximately 30 min); finally, at $950\text{ }^{\circ}\text{C}$, the

153 carrier gas was automatically switched to air and the sample was maintained at 950 °C until total
154 stabilization of the weight. The mass loss observed around 105 °C is attributed to moisture; the
155 mass loss registered from the end of this first step up to the switching of the carrier gas
156 corresponds to volatile matter; the mass loss comprised between the introduction of the air flow
157 and the stabilization of the weight is attributed to fixed carbon content; and lastly the final
158 residue corresponds to ash content (Valenzuela and Bernalte, 1985).

159 **2.2.3. Elemental analysis**

160 Elemental analysis was determined for the precursors and for all carbon adsorbents. The
161 determination of the samples' content in C, H, N and S was performed in a LECO TruSpec
162 CHNS Micro analyser, using sulfamethazine as calibration standard. The percentage of oxygen
163 was calculated by difference, at a dry and ash free basis.

164 **2.2.4. Fourier transform infrared spectroscopy with attenuated total 165 reflectance (FTIR-ATR)**

166 FTIR-ATR spectra were acquired through a Shimadzu-IRaffinity-1, using an attenuated
167 total reflectance (ATR) module, with a nitrogen purge. The measurements were recorded in the
168 range of 600-4000 cm^{-1} wavenumbers, 4.0 of resolution, 128 scans and with atmosphere and
169 background correction. Both precursors and all produced carbons were analysed.

170 **2.2.5. Point of zero charge (PZC)**

171 The PZC was determined, for the produced carbon adsorbents, by the pH drift method
172 (Aldegs et al., 2008). Briefly, ten solutions of NaCl 0.1 M with pH ranging between 2 and 11
173 were prepared by adjusting the pH with HCl 0.05 M and 0.1 M and NaOH 0.05 M and 0.1 M.
174 After that, 10 mL of each solution were transferred to a polypropylene tube containing 2 mg of
175 carbon. Each carbon was shaken with the solutions of different initial pH (pH_i), at 40 rpm,
176 overnight at 25 °C in an overhead shaker (Heidolph, Reax 2). Later, the final pH (pH_f) was
177 measured. The ΔpH ($\text{pH}_f - \text{pH}_i$) was plotted versus pH_i and PZC was determined as the pH
178 value where the plot crosses the x-axis.

2.2.6. Determination of carbons' functional groups by Boehm's Titration

The quantification of functional groups present on carbons surface was determined by the Boehm's method (Boehm, 1994). Accordingly, each carbon was added to NaOH 0.05 M, NaHCO₃ 0.05 M, Na₂CO₃ 0.05 M or HCl 0.05 M solutions into polypropylene tubes at a final concentration of 10 g L⁻¹, under nitrogen atmosphere. The mixtures were then shaken inside a thermostatic incubator at 25 °C for 24 h. After, the supernatants were filtered and 25 mL of each one was titrated with 0.1 M HCl or 0.1 M NaOH solutions in order to quantify the total acid and basic functional groups, respectively. In addition, the different acidic groups were determined as follows: the amount of carboxyl groups was estimated by neutralization with NaHCO₃ solution; and the amount of phenols was estimated from the difference between the neutralization with NaOH and that determined for the Na₂CO₃ solution. Furthermore, NaOH and HCl solutions were standardized with C₈H₅KO₄ and Na₂CO₃, respectively, for the determination of their exact concentration.

2.2.7. Specific surface area (S_{BET})

S_{BET} and total micropore volume (W_0) were determined for carbon adsorbents by nitrogen adsorption isotherms, acquired at 77 K using a Micromeritics Instrument, Gemini VII 2380 after outgassing the materials overnight at 120 °C. S_{BET} was calculated from the Brunauer-Emmett-Teller equation (Brunauer et al., 1938) in the relative pressure range 0.01-0.1. Total pore volume (V_p) was estimated from the amount of nitrogen adsorbed at a relative pressure of 0.99. W_0 was determined by applying the Dubinin-Radushkevich equation (Marsh and Rand, 1970) to the lower relative pressure zone of the nitrogen adsorption isotherm.

2.2.8. Scanning electron microscopy (SEM)

SEM images were obtained at different magnitudes using a Hitachi SU-70 in order to observe the superficial morphology of the precursors and the produced carbon adsorbents. The magnifications applied were 300x, 1 000x, 3 000x, 10 000x, 30 000x and 50 000x.

2.3. Batch adsorption experiments

In order to test the adsorptive performance of the produced carbons for the removal of pharmaceuticals (namely CBZ and SMX) from water, kinetic and adsorption equilibrium experiments were made under shaking and batch conditions. In all tests, solutions with an initial drug concentration (C_i) of 5 mg L^{-1} were used. Generally, polypropylene tubes containing a known mass of carbon adsorbent together with the drug solution were shaken at 80 rpm in an overhead shaker (Heidolph, Reax 2) at $25 \text{ }^\circ\text{C}$. Experiments were run in triplicate. After shaking, each sample was filtered through Whatman PVDF Membrane Filters $0.22 \text{ }\mu\text{m}$ to stop the adsorption process. Resulting solutions were analysed by capillary electrophoresis, in order to determine the remaining drug concentration, as described in section 2.3.3. Testing controls, without adsorbents, were also made. Before carrying out kinetic and adsorption equilibrium experiments, preliminary tests were performed with all carbon adsorbents with the purpose of concluding about the materials that have the best adsorptive performances. Based on those studies, only RP800-HCl-H₃PO₄ and BP800-HCl-H₃PO₄ were selected to study their kinetical behaviour and define their isotherms in equilibrium conditions.

Ultra-pure water and a final effluent of a WWTP (after secondary treatment, as discharged into the environment) were used for preparing the drug solutions. The effluent was collected from the urban WWTP of *Costa de Lavos* (Figueira da Foz), Portugal; immediately after collection and to remove suspended matter, it was filtered through cellulose Supor-450 Membrane Disc Filters $0.45 \text{ }\mu\text{m}$ with a vacuum system. After filtration, the samples were stored in the dark at $4 \text{ }^\circ\text{C}$ until use, for a maximum period of 10 days. The collected effluent was characterized after filtration. The pH, conductivity and dissolved organic carbon (DOC) content were 7.31 , 0.26 ms cm^{-1} and $29.3 \pm 0.7 \text{ mg L}^{-1}$, respectively.

2.3.1. Kinetic adsorption studies

To study the adsorption kinetics of CBZ and SMX onto the selected carbons, a fixed mass concentration of the carbon adsorbent (g L^{-1}) was employed, varying the contact time

233 between carbon adsorbents and drug solutions (shaking times of 5, 15, 30, 60, 120 and 240
234 min). In tests with real effluents, additional shaking times of 8, 10, 14 and 18 h were carried out.
235 For tests with CBZ, the adsorbent mass concentrations used were 0.035 and 0.070 g L⁻¹ in ultra-
236 pure water and WWTP effluent, respectively. In the case of SMX, 0.035 and 0.30 g L⁻¹ of
237 adsorbent were respectively used for tests in ultra-pure and WWTP effluent. The amount of the
238 target pharmaceutical adsorbed onto the corresponding adsorbent at each shaking time, q_t (mg
239 g⁻¹), was calculated by a mass balance (Equation 1). The experimental data were fitted to the
240 pseudo-first (Lagergren, 1898) and pseudo-second order (Ho et al., 2000) kinetic models
241 (Equations 2 and 3, respectively) in order to determine the kinetic parameters of the
242 experiments.

$$243 \quad q_t = \frac{(C_i - C_t)}{m} \times V \text{ (Equation 1)}$$

$$244 \quad q_t = q_e (1 - e^{-k_1 t}) \text{ (Equation 2)}$$

$$245 \quad q_t = \frac{q_e^2 k_2 t}{1 + k_2 q_e t} \text{ (Equation 3)}$$

246 where t is shaking time (min), C_i is the initial concentration of drug (mg L⁻¹), C_t is the remaining
247 drug concentration (mg L⁻¹) after shaking during a time t , m is the mass of adsorbent (g), V is
248 the volume of solution (L), q_e refers to the amount of adsorbate per unit mass of adsorbent at
249 equilibrium (mg g⁻¹), k_1 is the pseudo-first order rate constant (min⁻¹) and k_2 is the pseudo-
250 second order rate constant (g mg⁻¹ min⁻¹). GraphPad Prism 5 was used for the nonlinear
251 regression fittings of q_t versus t and three fitting parameters (R^2 , ASS and $S_{y/x}$) were determined
252 to evaluate the goodness of fit.

253

254 **2.3.2. Equilibrium adsorption studies**

255 These experiments were performed using the shaking time needed to attain the
256 equilibrium, as determined in section 2.3.1, varying the concentration of carbon adsorbents. The
257 amount of the target pharmaceutical adsorbed onto the corresponding adsorbent q_e (mg g⁻¹), was
258 determined by a mass balance (Equation 4) and the experimental data were fitted to the
259 Langmuir (Langmuir, 1916), Freundlich (Freundlich, 1906) and Langmuir-Freundlich (Sips,

260 1948) equilibrium models (Equations 5, 6 and 7, respectively) in order to determine the
261 equilibrium parameters of the systems.

$$262 \quad q_e = \frac{(C_i - C_e)}{m_{ads}} \times V \quad (\text{Equation 4})$$

$$263 \quad q_e = \frac{q_m \times K_L \times C_e}{1 + K_L \times C_e} \quad (\text{Equation 5})$$

$$264 \quad q_e = K_F \times C_e^{(1/n)} \quad (\text{Equation 6})$$

$$265 \quad q_e = \frac{q_{\max LF} \times K_{LF} C_e^{N_{LF-1}}}{1 + K_{LF} C_e^{N_{LF-1}}} \quad (\text{Equation 7})$$

266 where q_m is the maximum adsorbed concentration of adsorbate at the equilibrium (mg g^{-1}), C_e
267 refers to the concentration of adsorbate in the liquid phase at equilibrium (mg L^{-1}), K_L is the
268 Langmuir equilibrium constant (L mg^{-1}), K_F is the Freundlich equilibrium constant ($\text{mg g}^{-1} (\text{L}$
269 $\text{mg}^{-1})^{1/n}$), n and N_{LF} are the degrees of non-linearity, $q_{\max LF}$ (mg g^{-1}) represents the Langmuir-
270 Freundlich maximum adsorption capacity and K_{LF} ($\text{mg g}^{-1} (\text{mg L}^{-1})^{-1/N_{LF}}$) is the affinity
271 coefficient of Langmuir-Freundlich model. GraphPad Prism 5 was used for the nonlinear
272 regression fittings of q_e versus C_e and three fitting parameters (R^2 , ASS and $S_{y/x}$) were
273 determined to evaluate the goodness of fit.

274

275 **2.3.3. Drug quantification**

276 The quantification of CBZ and SMX was performed by capillary electrophoresis, using
277 a Beckman P/ACE MDQ (Fullerton, CA, USA) instrument, equipped with a UV/visible detector
278 and controlled by the software 32 Karat. The separation was made using a coated fused silica
279 capillary of 40 cm total length (30 cm to the detection window) using a MEKC (micellar
280 electrokinetic chromatography), as described in Calisto et al., 2015. Three replicates were run
281 for all experiments. Detailed experimental conditions (coating step, analysis parameters and
282 separation method for drug quantification) are presented in Table 1 of Supporting information
283 (SI).

284 The concentration of CBZ and SMX was determined using a calibration curve in the
285 range between 0.25 and 5.0 mg L⁻¹. Seven standard solutions of each drug were prepared (0.25,
286 0.50, 1.0, 2.0, 3.0, 4.0 and 5.0 mg L⁻¹) and three replicates of each standard solution were
287 analysed. A linear calibration curve for each new capillary was obtained using the least-squares
288 linear regression.

289

290 **3. Results and Discussion**

291 **3.1. Thermogravimetric analysis of the precursors and production of carbon** 292 **adsorbents**

293 The thermogravimetric analysis of carbon precursors (RP and BP) was made to
294 determine the mass loss profiles of the pulps and then choose the pyrolysis temperature for each
295 material. The results are presented in Figure S1 of Supporting Information (SI), which shows
296 two stages of mass loss during the pyrolysis of each RP and BP. The first derivative
297 thermogravimetric (DTG) peak of each pulp (76 °C for RP and 72 °C for BP) corresponds to the
298 mass loss derived from water evaporation and the second peaks (333 °C for RP and 356 °C for
299 BP) are due to the decomposition of organic matter. From these results, it was decided to carry
300 out the pyrolysis of both RP and BP at 500 °C to ensure the transformation of the organic
301 matter. Moreover, for comparison purposes, pyrolysis of RP and BP was also carried out at 800
302 °C because higher temperatures usually translate into a higher development of microporosity, as
303 observed in section 3.2, which is advantageous for adsorbents with superior adsorption capacity
304 (Calisto et al., 2014).

305 The production yield of all carbon adsorbents was calculated both before and after acid
306 washing. The yields obtained for RP and BP-based carbons varied between 18% and 25% for
307 non-activated and non-washed carbons and between 14% and 21% for non-activated washed
308 carbons, with BP-based carbons registering average yields slightly lower than RP-based
309 carbons. The small decrease verified between non-washed and washed non-activated carbons
310 indicate a low content of inorganic matter (removed by the acidic washing). The largest

311 differences were observed between AC produced from different activating agents, with
312 production yields of 21% and 17% for RP and BP H₃PO₄-ACs, respectively, and 4% and 5% for
313 RP and BP K₂CO₃-ACs, respectively.

314 **3.2. Physical and chemical characterisation of raw materials and carbon adsorbents**

315 TOC results (Table S2 of SI) highlight the low inorganic carbon content present in all
316 produced materials [$< 0.6\%$ (*w/w*)], even for non-washed carbons. This constitutes a great
317 advantage for the utilization of these pulps as precursors for carbon adsorbents, considering that
318 AC with high content in inorganic matter often implies lower surface areas and thus lower
319 performance. The TOC of the precursors (between 38 and 40%) highly increased after
320 pyrolysis, reaching contents between 76 and 83% for both non-washed and washed non-
321 activated carbons; and between 59 and 62% for H₃PO₄-AC and 71% for K₂CO₃-AC. Therefore,
322 ACs have less organic carbon (in percentage) than the non-activated carbons; this fact could be
323 explained by the presence of other chemical elements in the surface of the materials (namely
324 oxygen), resulting from the activating agent used, that represent a significant part of material's
325 chemical structure.

326 From proximate and elemental analyses (Table 1), it can be verified a decrease of
327 volatile matter with the increase of pyrolysis temperature, meaning that the carbons produced at
328 higher temperatures released more volatile matter and had more potential for the development
329 of porosity (namely, microporosity). It is also possible to conclude that BP has more potential to
330 develop a porous structure than RP due to its higher content in volatile matter. These facts were
331 proven by the results of S_{BET} and total volume of pores and micropores (Table 2). The presence
332 of a significant percentage of ashes in H₃PO₄-ACs (20.48% for RP800-HCl-H₃PO₄ and 16.55%
333 for BP800-HCl-H₃PO₄) means that activation with H₃PO₄ and pyrolysis of both RP and BP
334 generate a big amount of inorganic material that is not completely removed by the acid washing.
335 A high percentage of ashes in carbon's surface is generally a disadvantage for the carbons
336 because it decreases the adsorptive performance of the materials. However, these values are still
337 lower than those obtained by Jaria et al. (2015) for AC produced by the KOH or NaOH
338 activation of primary sludge, which had about 50% of ashes (*wt.%* dry basis) but showed large

339 adsorption capacities for the antidepressant fluoxetine. Regarding the elemental analysis, shown
340 in Table 1, it may be concluded that both precursors and carbon adsorbents are mostly
341 constituted by C and O, containing less than 6% of H and negligible amounts of N. The
342 materials have no S in their composition.

343 The FTIR-ATR spectra of RP, BP and of the produced carbon adsorbents are presented
344 in Figure S2 of SI. The spectra of RP and BP present typical bands of cellulose: bands at ~1030,
345 1105 and 1160 cm^{-1} , corresponding to cellulosic ethers (C-O-C bonds); band at ~1053 is
346 attributed to C-OH stretch of primary alcohols and carbohydrates (Boehm, 1994; Marsh and
347 Rand, 1970). All these bands disappeared in the materials pyrolysed at 500 °C. This is consistent
348 with the thermogravimetric results of the precursors (Figure S1 of SI), where the decomposition
349 of the most thermo-labile fraction of organic matter, as cellulose, occurs between 300 and 400
350 °C. There are also two bands in BP and RP spectra that are eliminated with pyrolysis: ~2890 and
351 3330 cm^{-1} which represent C-H stretch vibrations and -OH phenol, respectively (Ahmad et al.,
352 2007). In carbon adsorbent materials, several bands between 1660 and 2000 cm^{-1} appeared,
353 which are related with the presence of some aromatic combination bands (Coates, 2006). The
354 bands at ~1508 and 1339 cm^{-1} correspond to aromatic ring stretches (Marsh and Rand, 1970;
355 Yang et al., 2007). All bands in this region are typical of the presence of aromatic groups, which
356 constitute the main structure of AC. The presence of some bands at 3400-4000 cm^{-1} region in all
357 produced carbons is also notable and related with OH stretching (Yang et al., 2007).

358 The PZC was determined in order to know the net charge of each carbon (see Figure S3
359 of SI). Also, the concentration of some functional groups, namely carboxyl, phenols and total
360 basic groups were obtained through Boehm's Titration. Figure 1 relates the PZC with the
361 obtained functional groups concentrations for all produced carbon adsorbents. Since carboxyls
362 and phenols are acidic groups, the low PZCs is directly connected with the presence of high
363 concentrations of these two functional groups. On the other hand, higher PZCs are linked to a
364 higher concentration of total basic groups and lower concentration of both carboxyl and phenol
365 groups.

366 The S_{BET} results (Table 2) revealed large differences between non-activated and ACs,
367 highlighting the importance of the activation step in the development of higher porosity and
368 S_{BET} . Except for those activated with K_2CO_3 , all the carbons produced in the same conditions
369 presented higher S_{BET} for BP-based carbons, compared with RP-based carbons. This fact may be
370 explained by the higher content of volatile matter in BP in comparison with RP, as mentioned
371 before. It is noteworthy that, despite similar S_{BET} , H_3PO_4 -ACs have a microporous volume (W_0)
372 much higher than K_2CO_3 -ACs, which will certainly influence the adsorptive capacity of these
373 materials. For comparison purposes, the results determined for a commercially available AC
374 (PBFG4, kindly provided by Chemviron Carbon) were also included in Table 2. A complete
375 physical and chemical characterization of PBFG4 can be found in previous works (Calisto et al.,
376 2014; Jaria et al., 2015). As it may be seen, S_{BET} values for the ACs produced in this study are
377 very close or even higher (in the case of BP800- H_3PO_4 -HCl) than that of PBFG4. However, W_0
378 is significantly higher for the commercial AC (PBFG4) than for the here produced adsorbents.

379 The SEM analysis of the raw materials and produced carbon adsorbents are presented in
380 Tables S3-S6 of SI at different magnifications. Figures 2 and 3 present images of both
381 precursors and some examples of RP and BP-based carbons. The images show a gradual
382 difference between the surface morphology of the precursors, where the cellulose fibres are
383 intact, and the non-activated and non-washed carbons, where the fibres exhibit some degree of
384 destruction with no evident porosity (as confirmed by S_{BET} analysis) and finally the AC, where a
385 much more modified surface and a well-developed porosity are observable. This fact is
386 consistent with the results of S_{BET} , V_p and W_0 . Regarding ACs, it is possible to verify a huge
387 difference in the morphology between carbons activated with K_2CO_3 and with H_3PO_4 . K_2CO_3 -
388 ACs have a rough surface with a very noticeable porosity while H_3PO_4 -ACs have a smoother
389 surface, giving the impression that the fibres of the raw materials were barely affected. Still,
390 both activating agents resulted in carbon adsorbents with similar S_{BET} , with H_3PO_4 -ACs having
391 a much higher microporous volume. A possible explanation for the non-observed porosity in
392 H_3PO_4 -ACs SEM images could be the existence of a high number of micropores in these
393 carbons, when compared with K_2CO_3 -ACs, which are not visible at the used magnification.

394

395 **3.3. Batch adsorption experiments**

396 Preliminary tests, performed in ultra-pure water, revealed no adsorption of the studied
397 pharmaceuticals onto the non-ACs, even at mass concentrations up to 10 times higher than those
398 used for the same tests with ACs. This performance is, in fact, in accordance to S_{BET} results.
399 Therefore, kinetic and equilibrium studies were not performed with non-ACs.

400 Concerning the performance of the produced ACs in the preliminary experiments,
401 H_3PO_4 -ACs systematically presented better percentages for CBZ and SMX removal than
402 K_2CO_3 -ACs. Better removal percentages of H_3PO_4 -ACs should be related with the total pore
403 and micropore volumes, which are much higher than those obtained for K_2CO_3 -ACs (Table 2).
404 Moreover, the lower PZCs and a more acidic carbon surface may also be determinant factors for
405 a better performance, since H_3PO_4 -ACs have higher concentrations of carboxyl and phenol
406 groups in their structure, in comparison with K_2CO_3 -ACs (Figure 1). Based on these results, it
407 was decided to use the two H_3PO_4 -ACs (RP800-HCl- H_3PO_4 and BP800-HCl- H_3PO_4) to perform
408 the kinetic and equilibrium studies.

409

410 **3.3.1. Kinetic adsorption studies**

411 Kinetic studies for the adsorption of CBZ and SMX onto RP800-HCl- H_3PO_4 and
412 BP800-HCl- H_3PO_4 were performed in ultra-pure water and in WWTP effluents. The amount of
413 CBZ and SMX adsorbed (q_t , mg g^{-1}) is represented *versus* shaking time (t) in Figure 4.

414 The parameters determined by the fittings of kinetic models (Equations 2 and 3) to
415 experimental results are summarized in Table 3. For the fitting parameters, R^2 , $S_{y/x}$ and ASS,
416 pseudo-second order was the model that best fitted the experimental results on the adsorption of
417 both CBZ and SMX. Then, it was possible to conclude that the adsorption of both CBZ and
418 SMX was much faster (higher k_2) in ultra-pure water than in the WWTP effluent. It was also
419 proven that the difference between the adsorption kinetics in ultra-pure water and WWTP
420 effluents was more noticeable in tests with CBZ than with SMX. In fact, CBZ adsorption onto

421 RP800-H₃PO₄-HCl and BP800-H₃PO₄-HCl was ten and thirteen times faster, respectively, in
422 ultra-pure water than in WWTP effluents. These results are probably related to the complex
423 chemical composition of the secondary WWTP effluent, which contains organic and inorganic
424 components (such as dissolved organic matter) that can compete for the adsorption sites of the
425 carbons and, in this way, decrease the adsorption kinetics and hamper the access to the pores of
426 the adsorbents. In tests with SMX, BP800-H₃PO₄-HCl adsorbed just twice faster in ultra-pure
427 water, while RP800-H₃PO₄-HCl displayed faster adsorption kinetics in WWTP effluents.
428 Regarding the produced ACs, adsorption of both CBZ and SMX was faster (please, see higher
429 k_2 in Table 3) onto BP800-H₃PO₄-HCl than onto RP800-H₃PO₄-HCl either from ultra-pure
430 water or from the WWTP effluent.

431 The comparison of adsorption kinetics of the here produced adsorbents with a literature
432 study, that used, under the same experimental conditions, a commercial AC (PBFG4) for the
433 removal of CBZ and SMX from ultra-pure water (see Table 3) (Calisto et al., 2015), revealed
434 that the adsorption kinetics were faster for BP800-H₃PO₄-HCl (higher k_2), proving the good
435 potential of this type of precursors to produce ACs with good adsorptive properties.

436

437 **3.3.2. Equilibrium adsorption studies**

438 Equilibrium adsorption tests were performed for CBZ and SMX, both in ultra-pure
439 water and WWTP effluents. The amount of CBZ and SMX adsorbed (q_e , mg g⁻¹), both in ultra-
440 pure water and WWTP effluents, is represented *versus* the remaining concentration of drug in
441 solution (C_e) in Figure 5. The parameters obtained from the fittings of experimental results to
442 the considered equilibrium models (Equations 5, 6 and 7) are summarized in Table 3.

443 The best fit was obtained for the Langmuir-Freundlich equilibrium model, according to
444 the three selected fitting parameters (R^2 , $S_{y/x}$ and ASS) displayed in Table 3. From the analysis
445 of the fitted parameters for the Langmuir-Freundlich equilibrium model, it is possible to
446 conclude that, except for SMX adsorption onto RP800-HCl-H₃PO₄ from ultra-pure water, the
447 maximum adsorptive capacities (q_m) were always higher for BP-based ACs than for RP-based

448 ACs. These results are partially justified by the higher S_{BET} of BP800-HCl-H₃PO₄ (965 m² g⁻¹),
449 comparing with RP800-HCl-H₃PO₄ (768 m² g⁻¹). On the other hand, equilibrium experiments in
450 ultra-pure water present better or similar q_m for SMX than for CBZ. Contrarily, in WWTP
451 effluents, q_m was significantly higher for CBZ than for SMX. In any case, for these drugs, the
452 adsorptive capacity of both BP800-HCl-H₃PO₄ and RP800-HCl-H₃PO₄ was higher in ultra-pure
453 water than in real effluents due to the presence of organic matter or other competitors in the
454 latter. Yet, the decrease of carbons adsorptive capacity in WWTP effluent was much more
455 noticeable for SMX than for CBZ. In the case of CBZ, the adsorptive capacities of the
456 adsorbents just decreased 45% and 14%, using RP800-HCl-H₃PO₄ and BP800-HCl-H₃PO₄,
457 respectively, while for SMX, the adsorptive capacities decreased 92% and 87% for the same
458 carbon adsorbents, respectively. It was hypothesised that the reason for this accentuated
459 decrease may lie in the carbon surface chemistry. Since the PZC of H₃PO₄-ACs is quite low (2.3
460 for BP800-HCl-H₃PO₄ and 2.8 for RP800-HCl-H₃PO₄) and the pH of collected WWTP effluent
461 was 7.31, the functional groups present in the carbon surface are deprotonated, resulting in a
462 negatively charged carbon, attracting cations and repulsing anions. Due to the pH of the WWTP
463 effluent, SMX was negatively charged in these tests (pK_{a1}=1.8; pK_{a2}=5.7 (Calisto et al., 2015)),
464 which induced a repulsion between the drug and the groups present on the carbon surface,
465 making difficult the adsorption process. The dissociation equilibrium and speciation diagram of
466 SMX are schematized in Figure 6.

467 In ultra-pure water, which has a more acidic pH than WWTP effluents (between 5.5 and
468 6.0), there is an equilibrium between the neutral and negative species of SMX because pK_{a2} of
469 SMX is 5.7. With the presence of the neutral form of SMX, no electrostatic repulsion forces
470 between the neutral drug and the adsorbent surface occur, which further potentiates the
471 adsorption in this matrix. Then, the absence of competitors in ultra-pure water also favours the
472 SMX adsorption onto the produced carbon adsorbents.

473 The pH-dependent effect was not felt in CBZ adsorption experiments because CBZ has
474 a neutral charge at both the pH of ultra-pure water and WWTP effluents (pK_a=13.9 (Calisto et
475 al., 2015)). Therefore, in this case, the observed differences between the adsorption capacities

476 obtained between ultra-pure water and WWTP effluents are mainly due to the competition
477 effect of substances present in the effluents.

478 For comparison purposes, the results obtained under the same experimental conditions
479 for the removal of CBZ and SMX from ultra-pure water with a commercial AC (PBFG4)
480 (Calisto et al., 2015), are summarized in Table 3. The results show that the adsorption capacities
481 obtained with PBFG4 and the carbon adsorbents produced in this work are quite similar,
482 particularly in the case of BP800-H₃PO₄-HCl. Therefore, despite the total microporous volume
483 of PBFG4 being three times higher than that of BP800-H₃PO₄-HCl (please see Table 2),
484 maximum adsorption capacities of PBFG4 were only 1.2 and 1.1 times higher than those of
485 BP800-H₃PO₄-HCl for CBZ and SMX, respectively.

486 On the basis of the kinetic and equilibrium results, it is possible to conclude that BP800-
487 H₃PO₄-HCl was, among the here produced materials, the carbon adsorbent with the best
488 adsorptive performance, being comparable to that of a commercial AC used under identical
489 experimental conditions.

490

491 **4. Conclusions**

492 This study evaluated the adequacy of RP and BP as alternative and renewable-origin
493 precursors to produce high efficiency carbon adsorbents to remove pharmaceuticals from water.
494 The results obtained revealed that non-ACs produced from RP and BP have no potential for this
495 application, with negligible microporous structure and no ability to remove the tested
496 pharmaceuticals from ultra-pure water. On the other hand, the activation of RP and BP with
497 K₂CO₃ and H₃PO₄ allowed to produce carbon adsorbents with high adsorptive performances for
498 CBZ and SMX, with interesting physical and chemical characteristics such as a high S_{BET} and a
499 high total volume of pores and micropores, mainly for BP800-HCl-H₃PO₄ (S_{BET} of 965 m² g⁻¹,
500 V_p and W_0 of 0.41 and 0.11 cm², respectively). By studying the kinetic and equilibrium
501 behaviour of H₃PO₄-ACs for the adsorption of CBZ and SMX in ultra-pure water and WWTP
502 effluents, it was possible to conclude that the adsorption was slower and the capacity lower in
503 the WWTP effluents than in ultra-pure water. Differences should be related to the presence of

504 competitors that influence the adsorption process in WWTP effluents and to pH effects,
505 particularly in the case of SMX. In general, among the produced adsorbents, the one from BP
506 and activated with H₃PO₄ (BP800-HCl-H₃PO₄) displayed the best adsorptive performance,
507 which was comparable to that of a commercial AC. Therefore, it was here proved the potential
508 of pulp as precursor to produce adsorbents with high performance, which opens a new research
509 line towards diversification in the paper industry.

510

511 **Acknowledgements**

512 This work was funded by FEDER through COMPETE 2020 and by national funds
513 through FCT by the research project PTDC/AAG-TEC/1762/2014. Thanks are due for the
514 financial support to CESAM (UID/AMB/50017-POCI-01-0145-FEDER-007638), to
515 FCT/MCTES through national funds (PIDDAC), and the co-funding by the FEDER, within the
516 PT2020 Partnership Agreement and Compete 2020. The work was also developed within the
517 scope of the project CICECO - Aveiro Institute of Materials, POCI-01-0145-FEDER-007679
518 (UID/CTM/50011/2013), financed by national funds through the FCT/MEC. Vânia Calisto
519 thanks FCT for her postdoctoral grant (SFRH/BPD/78645/2011). Marta Otero and Sérgio
520 Santos thank support by the FCT Investigator Program (IF/00314/2015 and IF/00973/2014,
521 respectively). The authors acknowledge the kind collaboration of Cláudia Guerreiro and Maria
522 Miguel from the company “Luságua” for support with effluent collection.

523 **References**

- 524 AENOR: Norma UNE 32002:1995. <http://www.aenor.es/>.
- 525 AENOR: Norma UNE 32019:1985. <http://www.aenor.es/>.
- 526 AENOR: Norma UNE 32004:1984. <http://www.aenor.es/>.
- 527 Ahmad, A., Loh, M., Aziz, J., 2007. Preparation and characterization of activated carbon from
528 oil palm wood and its evaluation on Methylene blue adsorption. *Dyes Pigments* 75, 263–
529 272.
- 530 Aldegs, Y., Elbarghouthi, M., Elsheikh, A., Walker, G., 2008. Effect of solution pH, ionic

531 strength, and temperature on adsorption behavior of reactive dyes on activated carbon.
532 Dyes Pigments 77, 16–23.

533 Antunes, M., Esteves, V.I., Guégan, R., Crespo, J.S., Fernandes, A.N., Giovanela, M., 2012.
534 Removal of diclofenac sodium from aqueous solution by Isabel grape bagasse. Chem. Eng.
535 J. 192, 114–121.

536 Azargohar, R., Dalai, A.K., 2008. Steam and KOH activation of biochar: Experimental and
537 modeling studies. Micropor. Mesopor. Mat. 110, 413–421.

538 Babel, S., 2003. Low-cost adsorbents for heavy metals uptake from contaminated water: a
539 review. J. Hazard. Mater. 97, 219–243.

540 Bahlmann, A., Brack, W., Schneider, R.J., Krauss, M., 2014. Carbamazepine and its metabolites
541 in wastewater: Analytical pitfalls and occurrence in Germany and Portugal. Water Res. 57,
542 104–114.

543 Bahlmann, A., Carvalho, J.J., Weller, M.G., Panne, U., Schneider, R.J., 2012. Immunoassays as
544 high-throughput tools: Monitoring spatial and temporal variations of carbamazepine,
545 caffeine and cetirizine in surface and wastewaters. Chemosphere 89, 1278–1286.

546 Bansal, R.C., Goyal, M., 2005. Activated carbon adsorption. Taylor & Francis Group.

547 Boehm, H.P., 1994. Some aspects of the surface chemistry of carbon blacks and other carbons.
548 Carbon 32, 759–769.

549 Brunauer, S., Emmett, P.H., Teller, E., 1938. Adsorption of gases in multimolecular layers. J.
550 Am. Chem. Soc. 60, 309–319.

551 Calisto, V., Bahlmann, A., Schneider, R.J., Esteves, V.I., 2011. Application of an ELISA to the
552 quantification of carbamazepine in ground, surface and wastewaters and validation with
553 LC–MS/MS. Chemosphere 84, 1708–1715.

554 Calisto, V., Ferreira, C.I.A., Oliveira, J.A.B.P., Otero, M., Esteves, V.I., 2015. Adsorptive
555 removal of pharmaceuticals from water by commercial and waste-based carbons. J.
556 Environ. Manage. 152, 83–90.

557 Calisto, V., Ferreira, C.I.A., Santos, S.M., Gil, M.V., Otero, M., Esteves, V.I., 2014. Production
558 of adsorbents by pyrolysis of paper mill sludge and application on the removal of

559 citalopram from water. *Bioresource Technol.* 166, 335–344.

560 Clara, M., Strenn, B., Kreuzinger, N., 2004. Carbamazepine as a possible anthropogenic marker
561 in the aquatic environment: investigations on the behaviour of Carbamazepine in
562 wastewater treatment and during groundwater infiltration. *Water Res.* 38, 947–954.

563 Coates, J., 2006. Interpretation of Infrared Spectra, A Practical Approach, in: *Encyclopedia of*
564 *Analytical Chemistry*. John Wiley & Sons, Ltd, Chichester, UK.

565 Confederation of European Paper Industries, 2014. Resource efficiency in the pulp and paper
566 industry: making more from our natural resources.

567 Dias, I.N., Souza, B.S., Pereira, J.H.O.S., Moreira, F.C., Dezotti, M., Boaventura, R.A.R., Vilar,
568 V.J.P., 2014. Enhancement of the photo-Fenton reaction at near neutral pH through the use
569 of ferrioxalate complexes: A case study on trimethoprim and sulfamethoxazole antibiotics
570 removal from aqueous solutions. *Chem. Eng. J.* 247, 302–313.

571 European Commission, 2013. Pulp and paper industry [WWW Document]. URL:
572 https://ec.europa.eu/growth/sectors/raw-materials/industries/forest-based/pulp-paper_en
573 (accessed 12.12.17).

574 Ferreira, C.I.A., Calisto, V., Otero, M., Nadais, H., Esteves, V.I., 2016. Comparative adsorption
575 evaluation of biochars from paper mill sludge with commercial activated carbon for the
576 removal of fish anaesthetics from water in Recirculating Aquaculture Systems. *Aquac.*
577 *Eng.* 74, 76–83.

578 Ferrera-Lorenzo, N., Fuente, E., Suárez-Ruiz, I., Ruiz, B., 2014. KOH activated carbon from
579 conventional and microwave heating system of a macroalgae waste from the Agar–Agar
580 industry. *Fuel Process. Technol.* 121, 25–31.

581 Flores-Cano, J.V., Sánchez-Polo, M., Messoud, J., Velo-Gala, I., Ocampo-Pérez, R., Rivera-
582 Utrilla, J., 2016. Overall adsorption rate of metronidazole, dimetridazole and diatrizoate on
583 activated carbons prepared from coffee residues and almond shells. *J. Environ. Manage.*
584 169, 116–125.

585 Freundlich, H., 1906. Over the adsorption in solution. *J. Phy. Chem.* 57, 385-470.

586 H. Jones, O.A., Voulvoulis, N., Lester, J.N., 2005. Human pharmaceuticals in wastewater

587 treatment processes. *Crit. Rev. Environ. Sci. Technol.* 35, 401–427.

588 Ho, Y.S., McKay, G., Wase, D.A.J., Forster, C.F., 2000. Study of the sorption of divalent metal
589 ions on to peat. *Adsorpt. Sci. Technol.* 18, 639–650.

590 Jain, A., Balasubramanian, R., Srinivasan, M.P., 2015. Production of high surface area
591 mesoporous activated carbons from waste biomass using hydrogen peroxide-mediated
592 hydrothermal treatment for adsorption applications. *Chem. Eng. J.* 273, 622–629.

593 Jaria, G., Calisto, V., Gil, M.V., Otero, M., Esteves, V.I., 2015. Removal of fluoxetine from
594 water by adsorbent materials produced from paper mill sludge. *J. Colloid Interface Sci.*
595 448, 32–40.

596 Jaria, G., Silva, C.P., Ferreira, C.I.A., Otero, M., Calisto, V., 2017. Sludge from paper mill
597 effluent treatment as raw material to produce carbon adsorbents: An alternative waste
598 management strategy. *J. Environ. Manage.* 188, 203–211.

599 Johnson, A.C., Keller, V., Dumont, E., Sumpter, J.P., 2015. Assessing the concentrations and
600 risks of toxicity from the antibiotics ciprofloxacin, sulfamethoxazole, trimethoprim and
601 erythromycin in European rivers. *Sci. Total Environ.* 511, 747–755.

602 Khalili, N., Vyas, J., Weangkaew, W., Westfall, S., Parulekar, S., Sherwood, R., 2002.
603 Synthesis and characterization of activated carbon and bioactive adsorbent produced from
604 paper mill sludge. *Sep. Purif. Technol.* 26, 295–304.

605 Kyzas, G.Z., Deliyanni, E.A., 2015. Modified activated carbons from potato peels as green
606 environmental-friendly adsorbents for the treatment of pharmaceutical effluents. *Chem.*
607 *Eng. Res. Des.* 97, 135–144.

608 Lagergren, S., 1898. About the theory of so-called adsorption of soluble substances. *Kungliga*
609 *Svenska Vetenskapsakademiens*, 24, 1-39.

610 Langmuir, I., 1916. The constitution and fundamental properties of solids and liquids. *J. Am.*
611 *Chem. Soc.* 38, 2221–2295.

612 Larcher, S., Yargeau, V., 2012. Biodegradation of sulfamethoxazole: current knowledge and
613 perspectives. *Appl. Microbiol. Biotechnol.* 96, 309–318.

614 Li, W.-H., Yue, Q.-Y., Gao, B.-Y., Wang, X.-J., Qi, Y.-F., Zhao, Y.-Q., Li, Y.-J., 2011.

615 Preparation of sludge-based activated carbon made from paper mill sewage sludge by
616 steam activation for dye wastewater treatment. *Desalination* 278, 179–185.

617 Maneerung, T., Liew, J., Dai, Y., Kawi, S., Chong, C., Wang, C.-H., 2016. Activated carbon
618 derived from carbon residue from biomass gasification and its application for dye
619 adsorption: Kinetics, isotherms and thermodynamic studies. *Bioresource Technol.* 200,
620 350–359.

621 Marsh, H., Rand, B., 1970. The characterization of microporous carbons by means of the
622 dubinin-radushkevich equation. *J. Colloid Interface Sci.* 33, 101–116.

623 Monte, M.C., Fuente, E., Blanco, A., Negro, C., 2009. Waste management from pulp and paper
624 production in the European Union. *Waste Manag.* 29, 293–308.

625 Nowicki, P., Kazmierczak, J., Pietrzak, R., 2015. Comparison of physicochemical and sorption
626 properties of activated carbons prepared by physical and chemical activation of cherry
627 stones. *Powder Technol.* 269, 312–319.

628 Orlandi, G., Civasotto, J., Machado, F.R.S., Colpani, G.L., Magro, J.D., Dalcanton, F., Mello,
629 J.M.M., Fiori, M.A., 2017. An adsorbent with a high adsorption capacity obtained from
630 the cellulose sludge of industrial residues. *Chemosphere* 169, 171–180.

631 Presas, T., 2011. The pulp and paper industry: intelligent use of raw materials, in: *European
632 Economic and Social Committee.* Brussels.

633 Ren, X., Zeng, G., Tang, L., Wang, J., Wan, J., Liu, Y., Yu, J., Yi, H., Ye, S., Deng, R., 2018.
634 Sorption, transport and biodegradation – An insight into bioavailability of persistent
635 organic pollutants in soil. *Sci. Total Environ.* 610-611, 1154-1163.

636 Rivera-Utrilla, J., Sánchez-Polo, M., Ferro-García, M.Á., Prados-Joya, G., Ocampo-Pérez, R.,
637 2013. Pharmaceuticals as emerging contaminants and their removal from water: a review.
638 *Chemosphere* 93, 1268–1287.

639 Saucier, C., Adebayo, M.A., Lima, E.C., Cataluña, R., Thue, P.S., Prola, L.D.T., Puchana-
640 Rosero, M.J., Machado, F.M., Pavan, F.A., Dotto, G.L., 2015. Microwave-assisted
641 activated carbon from cocoa shell as adsorbent for removal of sodium diclofenac and
642 nimesulide from aqueous effluents. *J. Hazard. Mater.* 289, 18–27.

643 Silva, T.L., Ronix, A., Pezoti, O., Souza, L.S., Leandro, P.K.T., Bedin, K.C., Beltrame, K.K.,
644 Cazetta, A.L., Almeida, V.C., 2016. Mesoporous activated carbon from industrial laundry
645 sewage sludge: Adsorption studies of reactive dye Remazol Brilliant Blue R. *Chem. Eng.*
646 *J.* 303, 467–476.

647 Sips, R., 1948. On the Structure of a Catalyst Surface. *J. Chem. Phys.* 16, 490–495.

648 Teixeira, S., Delerue-Matos, C., Santos, L., 2012. Removal of sulfamethoxazole from solution
649 by raw and chemically treated walnut shells. *Environ. Sci. Pollut. Res.* 19, 3096–3106.

650 Valenzuela, C., Bernalte, A., 1985. Un método termogravimétrico rápido para análisis
651 inmediato de carbones. *Boletín Geológico y Min.* 58–61.

652 Wei, L., Yushin, G., 2012. Nanostructured activated carbons from natural precursors for
653 electrical double layer capacitors. *Nano Energy* 1, 552–565.

654 Yang, H., Yan, R., Chen, H., Lee, D.H., Zheng, C., 2007. Characteristics of hemicellulose,
655 cellulose and lignin pyrolysis. *Fuel* 86, 1781–1788.

Tables

Table 1 – Proximate and elemental analyses for precursors and carbon materials

Sample	Proximate analysis (wt.%, dry basis)					Elemental analysis (wt.%, dry and ash free basis)				
	Moisture	Volatile Matter (VM)	Fixed Carbon (FC)	Ash	VM/FC	% C	% H	% N	% S	% O *
RP	6.13	79.77	19.29	0.94	4.14	41.60	5.93	-	-	52.47
BP	6.88	87.75	11.72	0.53	7.49	42.34	5.99	0.03	-	51.63
RP500	4.83	21.54	74.92	3.54	0.29	79.42	2.44	-	-	18.15
BP500	3.11	27.91	72.09	-	0.39	81.30	2.28	-	-	16.41
RP800	8.37	11.38	82.96	5.66	0.14	82.70	0.96	0.05	-	16.29
BP800	6.02	8.89	90.57	0.53	0.10	83.93	0.23	-	-	15.85
RP500-HCl	4.94	19.61	79.84	0.55	0.25	77.56	2.77	-	-	19.67
BP500-HCl	4.61	19.51	79.56	0.93	0.25	78.91	2.20	-	-	18.89
RP800-HCl	8.38	7.71	91.11	1.17	0.08	85.69	-	0.12	-	14.19
BP800-HCl	8.04	7.50	91.78	0.72	0.08	84.88	-	-	-	15.12
RP800-HCl-K ₂ CO ₃	14.92	11.72	87.84	0.44	0.13	72.79	-	-	-	27.21
BP800-HCl-K ₂ CO ₃	16.36	14.64	85.36	0.00	0.17	71.82	0.94	0.05	-	27.18
RP800-HCl-H ₃ PO ₄	17.67	23.96	55.56	20.48	0.43	68.93	1.69	-	-	29.38
BP800-HCl-H ₃ PO ₄	14.37	27.12	56.33	16.55	0.48	73.58	4.04	-	-	22.37

* - calculated by difference

Table 2 – Specific surface area (S_{BET}), total pore volume (V_p), total micropore volume (W_0) and average pore diameter (D) of all produced materials. For comparison purposes, data are also presented for PBF4, a commercially available AC (from Calisto et al., 2014).

Carbon adsorbent	S_{BET} (m^2g^{-1})	V_p (cm^3g^{-1})	W_0 (cm^3g^{-1})	D (nm)
RP500	3	0.002	0.000	19.00
BP500	6	0.010	0.000	7.26
RP800	3	0.003	0.001	7.90
BP800	5	0.001	0.000	9.43
RP500-HCl	6	0.004	0.001	5.95
BP500-HCl	27	0.009	0.001	5.18
RP800-HCl	27	0.003	0.001	5.17
BP800-HCl	56	0.010	0.001	5.20
RP800-HCl -K₂CO₃	855	0.065	0.018	2.69
BP800-HCl -K₂CO₃	814	0.056	0.015	2.66
RP800-HCl -H₃PO₄	768	0.311	0.137	2.33
BP800-HCl -H₃PO₄	965	0.408	0.108	2.59
PBF4 (Calisto et al., 2014)	848	0.360	0.295	0.84

Table 3 - Fitting parameters of pseudo-first and pseudo-second order kinetic models and of Langmuir, Freundlich and Langmuir-Freundlich equilibrium models for experimental results on the adsorption of CBZ and SMX, onto RP800-HCl-H₃PO₄ and BP800-HCl-H₃PO₄ in ultra-pure water and WWTP effluents.

		CBZ					SMX				
		Ultra-pure water		WWTP effluent			Ultra-pure water		WWTP effluent		
		RP800- H ₃ PO ₄ -HCl	BP800- H ₃ PO ₄ -HCl	PBFG4 (Calisto et al., 2015)	RP800- H ₃ PO ₄ -HCl	BP800- H ₃ PO ₄ -HCl	RP800- H ₃ PO ₄ -HCl	BP800- H ₃ PO ₄ -HCl	PBFG4 (Calisto et al., 2015)	RP800- H ₃ PO ₄ -HCl	BP800- H ₃ PO ₄ -HCl
Kinetic studies											
Pseudo 1 st order	q_e (mg g ⁻¹)	56±4	85±3	122±3	25±3	51±3	83±3	95±3	110±3	5.3±0.6	13.0±0.9
	k_1 (min ⁻¹)	0.01±0.03	0.26±0.06	0.10±0.01	0.006±0.002	0.015±0.004	0.058±0.007	0.19±0.037	0.15±0.02	0.017±0.007	0.021±0.006
	R^2	0.901	0.968	0.989	0.813	0.874	0.984	0.972	0.978	0.789	0.870
	$S_{y/x}$	7.375	6.234	5.349	4.165	6.945	4.602	6.622	6.674	1.025	1.829
	ASS	271.9	194.3	-	156.1	385.8	84.71	219.3	-	7.357	26.77
Pseudo 2 nd order	q_e (mg g ⁻¹)	61±3	90±2	132±3	29±3	56±3	90±2	101±2	117±3	6.0±0.6	14.0±0.8
	k_2 (g mg ⁻¹ min ⁻¹)	0.0030±0.0009	0.005±0.001	0.0011±0.0002	0.0003±0.0001	0.0004±0.0001	0.00089±0.00009	0.0030±0.0003	0.0021±0.0004	0.004±0.002	0.0020±0.0007
	R^2	0.960	0.990	0.993	0.862	0.935	0.996	0.996	0.991	0.876	0.936
	$S_{y/x}$	4.712	3.494	4.253	3.852	4.979	2.173	2.528	4.387	0.785	1.279
	ASS	111.0	61.04	-	115.4	198.3	18.89	31.95	-	4.314	13.10
Equilibrium studies											
Langmuir	q_m (mg g ⁻¹)	57±2	93±2	116±3	29.9±0.5	80±3	93±1	110±4	118±5	8.8±0.2	13.3±0.5
	K_L (L mg ⁻¹)	9±4	3.2±0.4	10±2	5.5±0.6	2.2±0.4	4.5±0.4	5.0±0.7	2.3±0.4	55±37	13±3
	R^2	0.972	0.991	0.9906	0.991	0.978	0.997	0.985	0.9819	0.987	0.961
	$S_{y/x}$	3.111	2.742	3.972	0.876	3.420	1.659	4.215	4.744	0.374	0.907
	ASS	67.74	52.64	-	6.905	105.3	19.27	124.3	-	0.838	5.759
Freundlich	K_F (mg L ^{-1/n} g ^{-1/n})	48±2	67±1	102.7±0.8	23.6±0.6	52±2	72.6±0.7	88±3	78±2	8.6±0.2	11.5±0.5
	n	12±5	4.0±0.4	9.1±0.7	6.0±0.9	3.6±0.4	5.3±0.3	5±1	3.1±0.2	67±92	10±4
	R^2	0.965	0.988	0.998	0.969	0.971	0.996	0.956	0.987	0.983	0.918
	$S_{y/x}$	3.479	3.144	2.011	1.620	3.918	1.828	7.213	4.031	0.426	1.317
	ASS	84.72	69.19	-	23.63	138.2	23.40	364.2	-	1.091	12.13
Langmuir - Freundlich	q_m (mg g ⁻¹)	54±4	107±21	Ambiguous fitting	30±1	92±19	106±14	102±4	Ambiguous fitting	8.7±0.2	13.0±0.6
	K_{LF} (mg g ⁻¹ (mg L ⁻¹) ^{1/n_{LF}})	12±19	2±1	Ambiguous fitting	5±2	1.4±0.7	2±1	11±6	Ambiguous fitting	1.38x10 ⁻⁶ ±9x10 ⁻⁸	22±25
	n_{LF}	0.8±0.8	1.4±0.5	Ambiguous fitting	1.1±0.2	1.4±0.4	1.6±0.5	0.7±0.2	Ambiguous fitting	0±7	0.8±0.4
	R^2	0.972	0.993	Ambiguous fitting	0.991	0.981	0.998	0.990	Ambiguous fitting	0.990	0.963

$S_{y/x}$	3.336	2.724	0.923	3.370	1.461	3.698	0.357	0.950
ASS	66.75	44.53	6.820	90.88	12.81	82.05	0.637	5.417

Figure Captions

Figure 1 – Point of zero charge (PZC) and functional groups concentrations of the produced carbon adsorbents

Figure 2 - SEM images of RP, RP-800 and RP800-HCl-K₂CO₃ (from left to right) at 10 000x

Figure 3 - SEM images of BP at 3 000x, BP-800 and BP800-HCl- H₃PO₄ at 10 000x (from left to right)

Figure 4 – Experimental kinetic results and nonlinear fittings of the pseudo-second order kinetic model (best fit) corresponding to the adsorption of CBZ and SMX onto RP800-HCl-H₃PO₄ and BP800-HCl-H₃PO₄, from ultra-pure water or WWTP effluents

Figure 5 – Experimental equilibrium results and nonlinear fittings of the Langmuir-Freundlich model (best fit) corresponding to the adsorption of CBZ and SMX onto RP800-HCl-H₃PO₄ and BP800-HCl-H₃PO₄, from either ultra-pure water or WWTP effluents

Figure 6 – Dissociation equilibrium and speciation diagram of SMX (adapted from Teixeira et al., 2012 and Dias et al., 2014)

Figure 1 b&w
[Click here to download high resolution image](#)

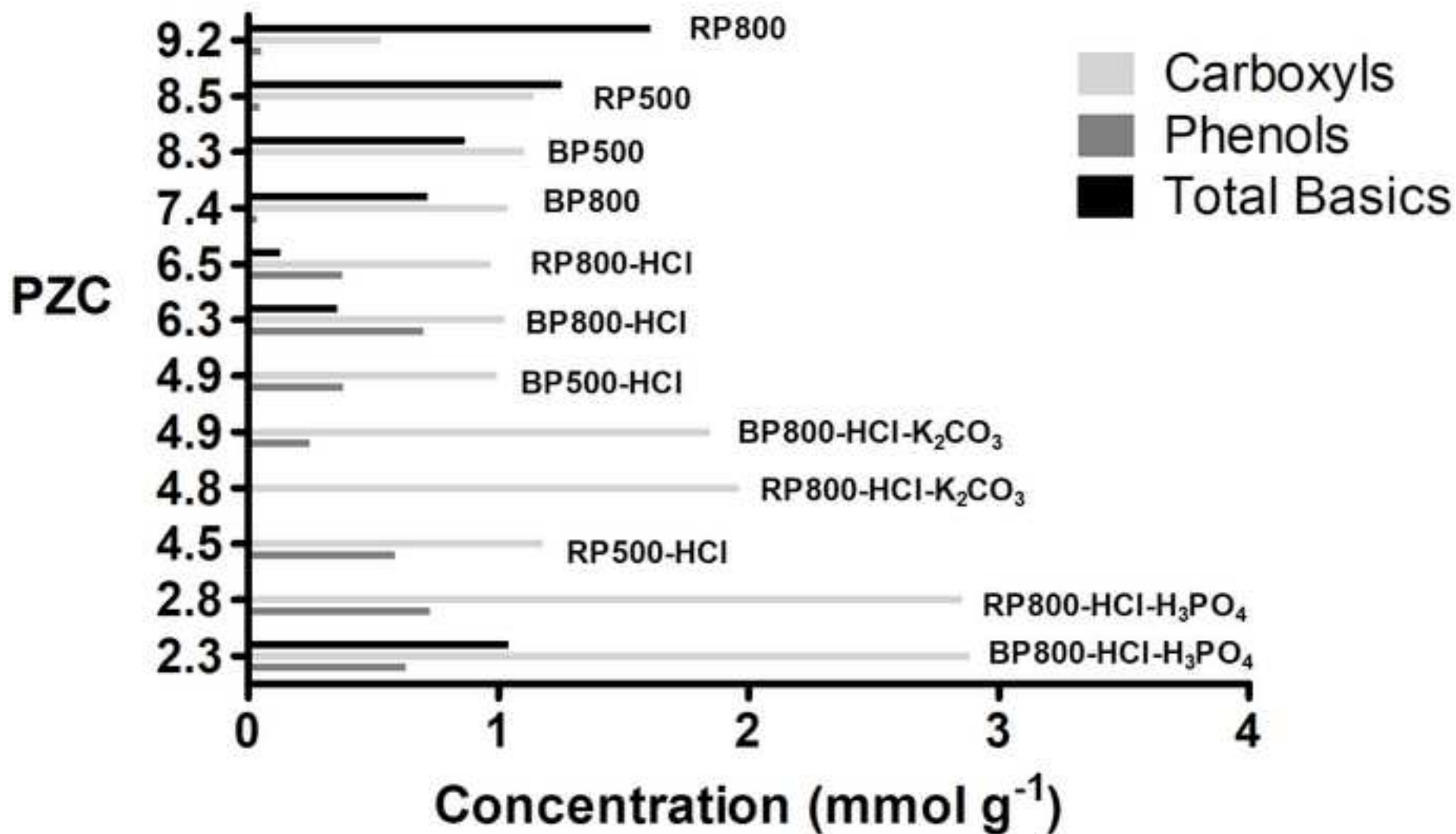


Figure 1 color
[Click here to download high resolution image](#)

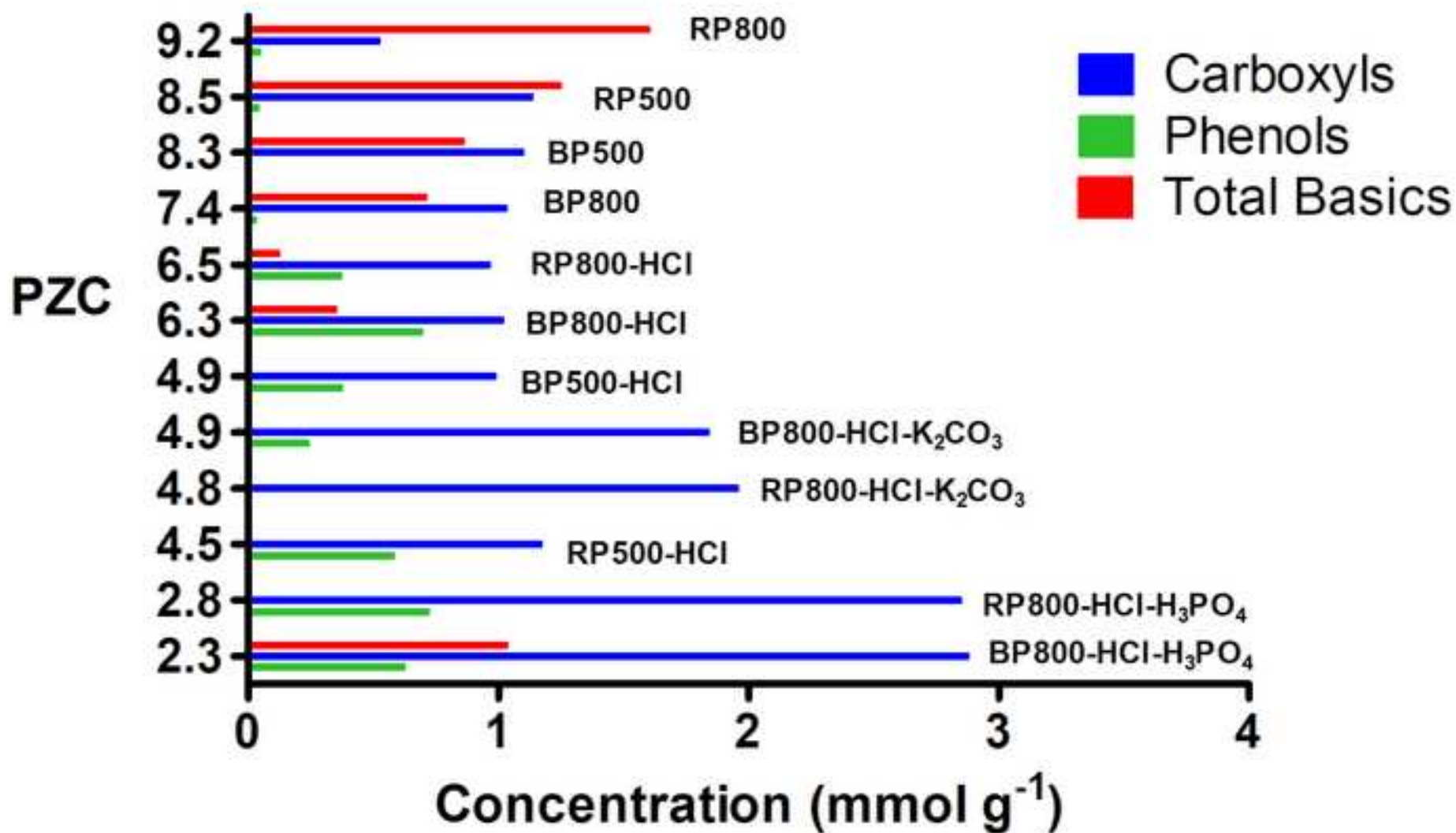


Figure 2
[Click here to download high resolution image](#)

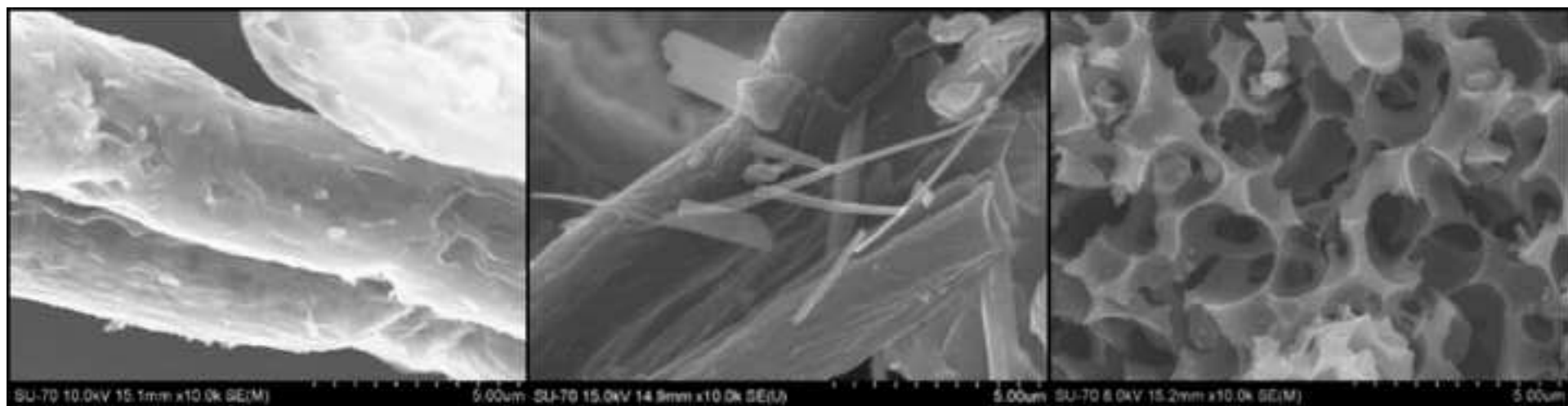


Figure 3
[Click here to download high resolution image](#)

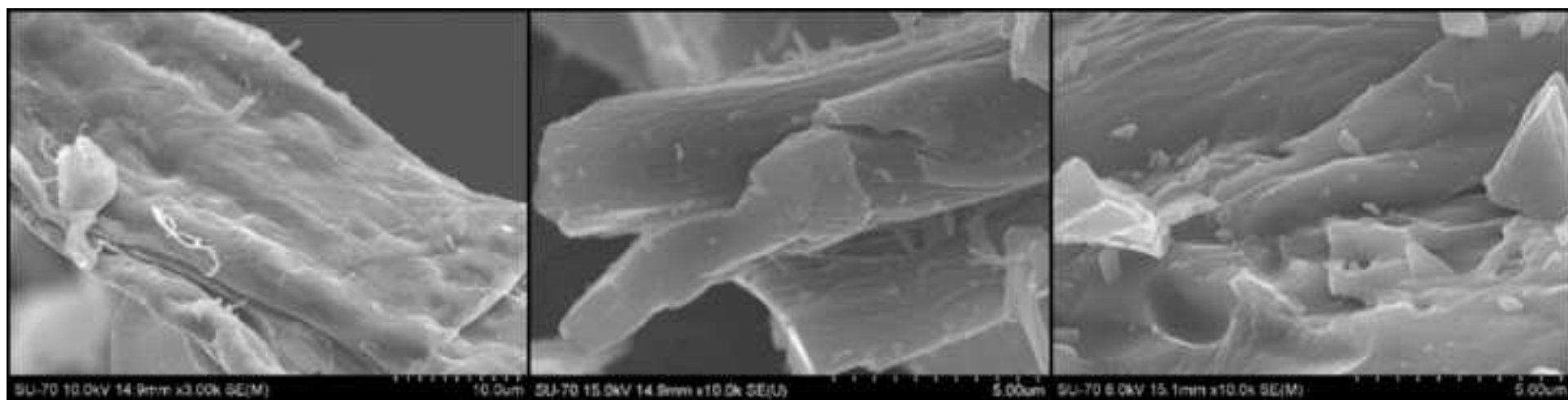


Figure 4 b&w
[Click here to download high resolution image](#)

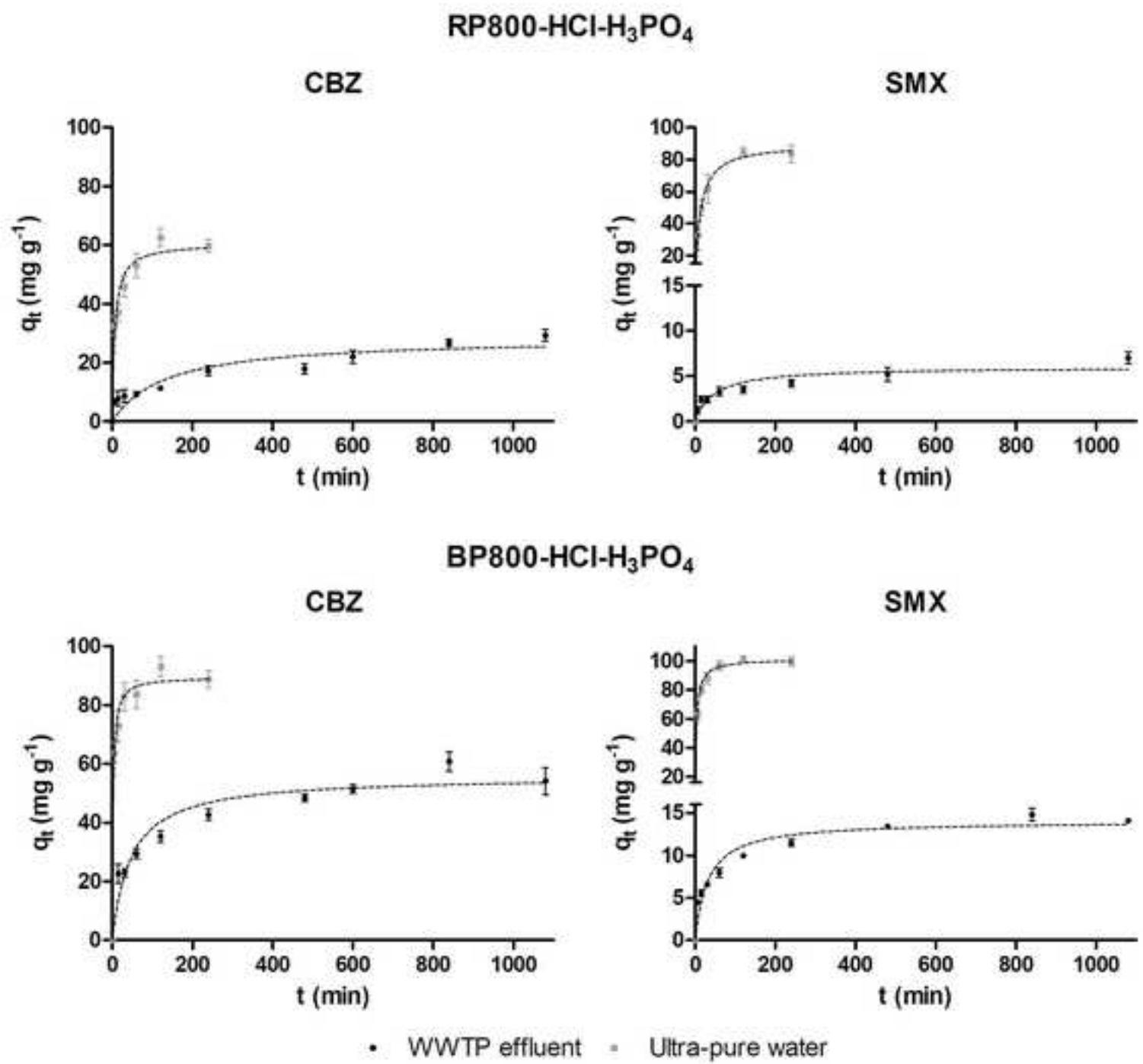


Figure 4 color
[Click here to download high resolution image](#)

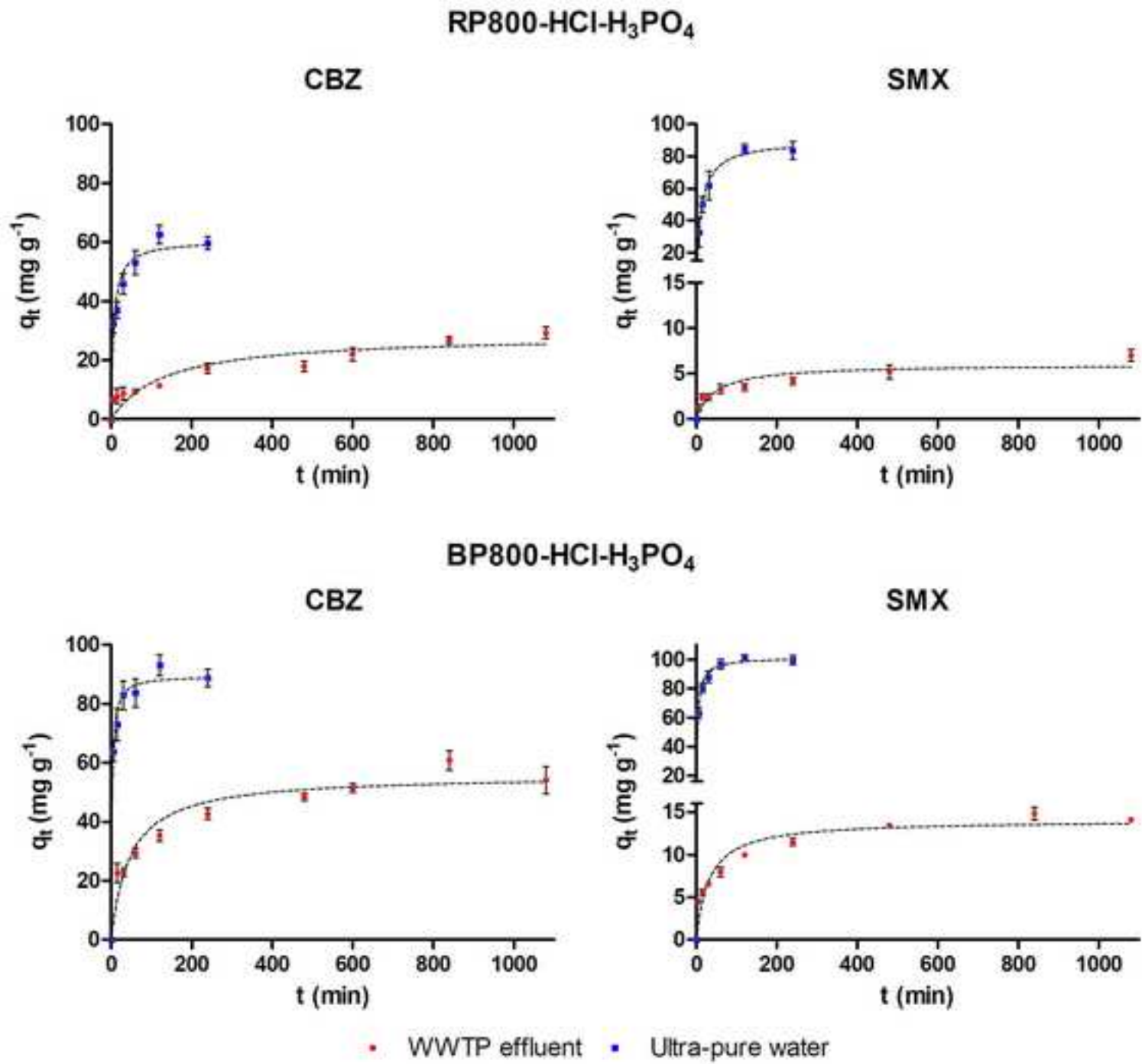


Figure 5 b&w
[Click here to download high resolution image](#)

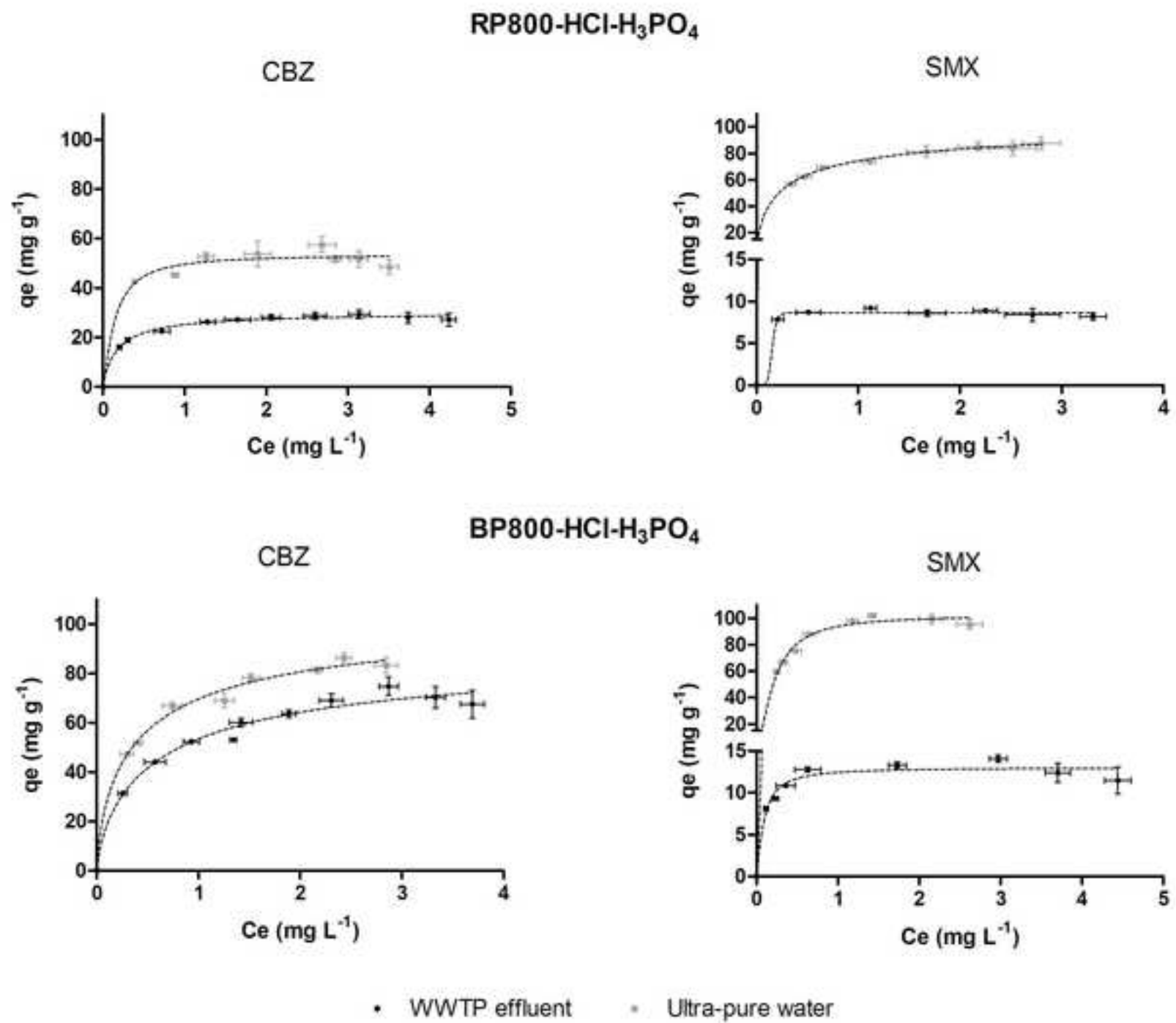


Figure 5 color
[Click here to download high resolution image](#)

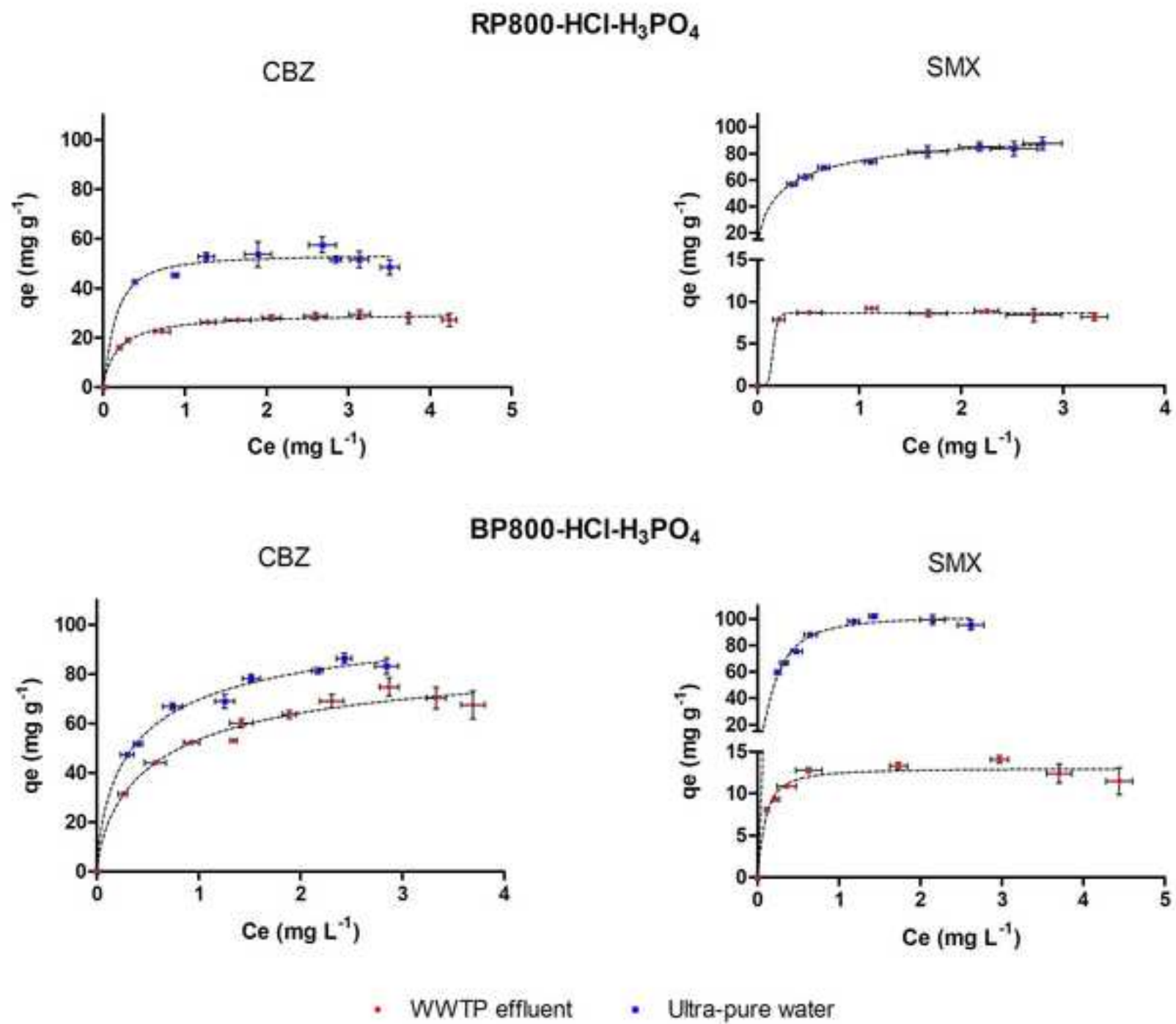
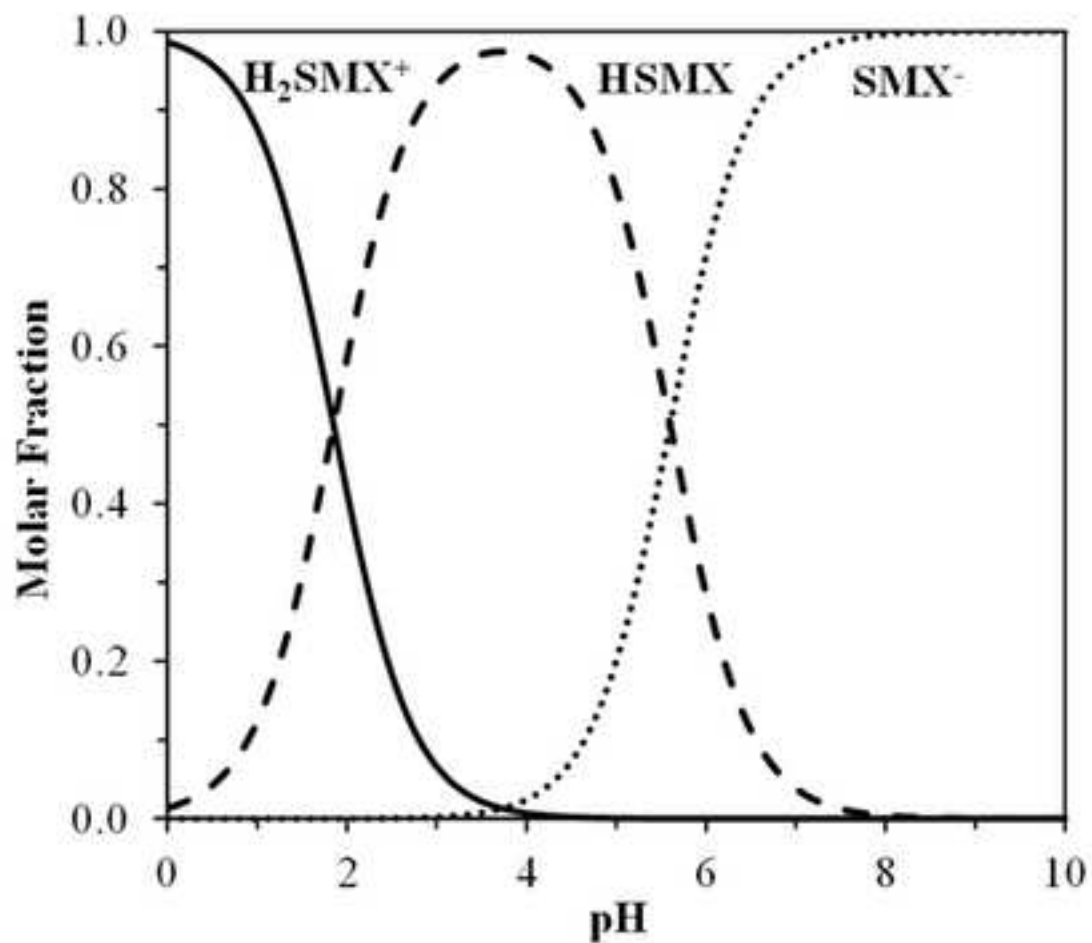


Figure 6
[Click here to download high resolution image](#)



Supplementary material for on-line publication only

[Click here to download Supplementary material for on-line publication only: Supporting_Information.docx](#)